




Mechanism of effective combination radio-immunotherapy against 9464D-GD2, an immunologically cold murine neuroblastoma

Taylor J Aiken ^{1,2}, Amy K Erbe,² Lauren Zebertavage,² David Komjathy,² Arika S Feils,² Matthew Rodriguez,² Ashley Stuckwisch,² Stephen D Gillies,³ Zachary S Morris,² Jen Birstler,⁴ Alexander L Rakhmilevich ², Paul M Sondel ^{2,5}

To cite: Aiken TJ, Erbe AK, Zebertavage L, *et al.* Mechanism of effective combination radio-immunotherapy against 9464D-GD2, an immunologically cold murine neuroblastoma. *Journal for ImmunoTherapy of Cancer* 2022;**10**:e004834. doi:10.1136/jitc-2022-004834

► Additional supplemental material is published online only. To view, please visit the journal online (<http://dx.doi.org/10.1136/jitc-2022-004834>).

Accepted 04 May 2022

ABSTRACT

Background Most pediatric cancers are considered immunologically cold with relatively few responding to immune checkpoint inhibition. We recently described an effective combination radio-immunotherapy treatment regimen (combination adaptive-innate immunotherapy regimen (CAIR)) targeting adaptive and innate immunity in 9464D-GD2, an immunologically cold model of neuroblastoma. Here, we characterize the mechanism of CAIR and the role of major histocompatibility complex class I (MHC-I) in the treatment response.

Methods Mice bearing GD2-expressing 9464D-GD2 tumors were treated with CAIR (external beam radiotherapy, hu14.18-IL2 immunocytokine, CpG, anti-CD40, and anti-CTLA4) and tumor growth and survival were tracked. Depletion of specific immune cell lineages, as well as testing in immunodeficient R2G2 mice, were used to determine the populations necessary for treatment efficacy. Induction of MHC-I expression in 9464D-GD2 cells in response to interferon- γ (IFN- γ) and CAIR was measured *in vitro* and *in vivo*, respectively, by flow cytometry and quantitative real-time PCR. A cell line with IFN- γ -inducible MHC-I expression (9464D-GD2-I) was generated by transfecting a subclone of the parental cell line capable of expressing MHC-I with GD2 synthase and was used *in vivo* to assess the impact of MHC-I expression on responsiveness to CAIR.

Results CAIR cures some mice bearing small (50 mm³) but not larger (100 mm³) 9464D-GD2 tumors and these cured mice develop weak memory responses against tumor rechallenge. Early suppression of 9464D-GD2 tumors by CAIR does not require T or natural killer (NK) cells, but eventual tumor cures are NK cell dependent. Unlike the parental 9464D cell line, 9464D-GD2 cells have uniformly very low MHC-I expression at baseline and fail to upregulate expression in response to IFN- γ . In contrast, 9464D-GD2-I upregulates MHC-I in response to IFN- γ and is less responsive to CAIR.

Conclusion Treatment with CAIR cures 9464D-GD2 tumors in a NK cell dependent manner and induction of MHC-I by tumors cells was associated with decreased efficacy. These results demonstrate that the early tumor response to this regimen is T and NK cell independent, but that NK cells have a role in generating lasting cures in

WHAT IS ALREADY KNOWN ON THIS TOPIC

⇒ A combination radio-immunotherapy regimen (external beam radiotherapy, hu14.18-IL2 immunocytokine, CpG, anti-CD40, and anti-CTLA4) is effective in immunologically cold 9464D-GD2 murine neuroblastoma.

WHAT THIS STUDY ADDS

⇒ Natural killer (NK) cells are a primary effector population responsible for the responsiveness of 9464D-GD2 tumors to combination radio-immunotherapy and their activity might be aided by very low expression of major histocompatibility complex class I on the surface of 9464D-GD2 cells. Further strategies to better inhibit tumor outgrowth may require further NK activation or the ability to engage alternative immune effector cells.

the absence of MHC-I expression by tumor cells. Further strategies to better inhibit tumor outgrowth in this setting may require further NK activation or the ability to engage alternative immune effector cells.

INTRODUCTION

Neuroblastoma is the most common extracranial solid tumor in pediatrics. High-risk cases, which account for approximately half of all patients, are associated with a 5-year overall survival rate of 50%.^{1,2} Tumor-specific monoclonal antibodies (mAb) targeting GD2, a disialoganglioside preferentially upregulated on tumors of neuroectodermal origin, including neuroblastoma and melanoma, are a component of standard therapy for high-risk neuroblastoma patients following combination chemotherapy, surgical resection, and autologous stem cell transplant.³ Despite this multimodal strategy, the risk of relapse remains high, highlighting an opportunity



© Author(s) (or their employer(s)) 2022. Re-use permitted under CC BY-NC. No commercial re-use. See rights and permissions. Published by BMJ.

For numbered affiliations see end of article.

Correspondence to

Dr Paul M Sondel;
pmsondel@humonc.wisc.edu

for an enhanced immunotherapeutic approach to reduce the risk of recurrence.

We previously described a combination radio-immunotherapy regimen, which activates components of both the adaptive and innate immune systems to induce tumor cures in an immunologically cold model of neuroblastoma.⁴ Herein, this combination adaptive-innate immunotherapy regimen is referred to as 'CAIR'. The foundation of this approach is the hu14.18-IL2 immunocytokine (IC), a fusion protein linking hu14.18 anti-GD2 mAb and interleukin (IL)-2. When immunocytokine is delivered intratumorally (IT-IC) in combination with local radiation therapy (12 Gy RT), this approach generates an in situ vaccination effect that cures mice bearing GD2-expressing B78 melanoma and NXS2 neuroblastoma.^{4,5} The treatment efficacy was enhanced by concurrent immune checkpoint inhibition with anti-CTLA4 antibodies.⁵ However, this RT + IT-IC approach is not effective, even when anti-CTLA4 is added, in mice bearing 9464D-GD2 neuroblastoma tumors, which are immunologically cold and are associated with low tumor mutation burden.⁴

Separately, we have described an effective combination of innate-targeting (agonistic anti-CD40 mAb and CpG-oligodeoxynucleotides) and adaptive-targeting (IT-IC and anti-CTLA4 mAb) approaches to cure tumors in a murine model of melanoma.⁶ When we added local RT to this treatment combination (ie, CAIR), it was able to cure some mice bearing 9464D-GD2 tumors.⁴ However, the key cellular mediators of CAIR and the relative importance of each component are not fully understood. In addition, there are limitations to this approach. First, in situ vaccination with RT and IT-IC results in protection against lung metastasis and rejection of tumor rechallenge in B78 melanoma.⁵ However, tumor cure of 9464D-GD2 neuroblastoma by CAIR fails to generate protective memory against tumor rechallenge, only slowing outgrowth of rechallenged 9464D-GD2 tumors, rather than preventing outgrowth.⁴ This incomplete memory suggests a less effective systemic adaptive response that may not treat distant 9464D-GD2 disease. Second, the development of CAIR required a dose reduction of hu14.18-IL2 in response to observed toxicity, suggesting that it is likely that this regimen could be associated with significant toxicity in patients.⁴ Understanding the mediators of efficacy in this combination immunotherapy regimen would allow for rational modifications that might improve the systemic immune response and decrease toxicity.

In this report, we identify key immune cell mediators responsible for the efficacy of CAIR (RT, IT-IC, anti-CD40, CpG, and anti-CTLA4) in mice bearing 9464D-GD2 neuroblastoma. Our data suggest that natural killer (NK) cells are a primary effector population responsible for the responsiveness of 9464D-GD2 tumors to CAIR and that their activity might be aided by very low expression of major histocompatibility complex class I (MHC-I) on the surface of 9464D-GD2 cells. Accordingly, we observed that increased MHC-I expression on tumors cells was

associated with worse treatment outcomes in GD2-expressing 9464D models, suggesting that CAIR-induced NK cell activity can be suppressed by tumor expression of MHC-I and that this regimen generates a T cell response that is insufficient to fully compensate for the suppression of NK cells by MHC-I.

METHODS

Cells

The parental 9464D cell line is a MYCN-driven neuroblastoma cell line derived from TH-MYCN transgenic mice.⁷ 9464D-GD2 is a GD2-expressing cell line derived from 9464D as previously described.⁴ A subclone of the parental 9464D cell line selected for interferon- γ (IFN- γ)-inducible MHC-I expression was obtained by flow sorting and was subsequently transfected to express GD2 and GD3 synthases (9464D-GD2-I). Cells were grown in DMEM supplemented with 10% fetal bovine serum, 2 μ M L-glutamine, 1 mM sodium pyruvate, 1X MEM non-essential amino acids, 100 U/mL penicillin, and 100 μ g/mL streptomycin. Cell lines were confirmed to be negative for mycoplasma by PCR prior to use.

Murine tumor models

All mice procedures were conducted in accordance with the Institutional Animal Care and Use Committee at the University of Wisconsin-Madison. C57BL/6 female mice aged 6–8 weeks were purchased from Taconic Biosciences (Germantown, New York, USA). R2G2 mice (B6;129-*Rag2*^{tm1Fwa}*IL2rg*^{tm1Rsky}/DwlHsd) were used for experiments requiring immunodeficient mice and were obtained from Envigo (Indianapolis, Indiana, USA). R2G2 mice are *Rag2* and *IL2RG* double knockout mice that are deficient in B, T, and NK cells and relatively radioresistant.^{8,9} 9464D-GD2 flank tumors were engrafted by intradermal flank injection of 2×10^6 tumor cells diluted in 100 μ L phosphate buffered saline (PBS). Tumor size was determined by precision caliper measurement, and tumor volume was approximated using the formula (tumor volume in $\text{mm}^3 = ((\text{tumor width in mm}^2) \times (\text{tumor length in mm}^2))$). Mice were randomized into treatment groups when tumors reached enrollment size (50 mm^3). The first day of treatment with RT was defined as 'day 1'. After injection, approximately 90% of mice had tumors at the time of randomization that were suitably uniform to enable similar tumor sizes among all randomized mice (ie, within the tumor volume range of 40–60 mm^3); the remaining 10% of mice were excluded from randomization.

Flank tumor rechallenge experiments were performed with tumor-free mice approximately 40 days after treatment start unless otherwise indicated. Rechallenge consisted of intradermal injection of 2×10^6 tumor cells on the contralateral flank from the original tumor cell injection. Tumor volume was assessed twice weekly and mice were euthanized when tumors exceeded 20 mm in any direction or mice were assessed to be in distress

by changes to posture, activity, or grooming. In experiments where rechallenge was conducted in the setting of a primary tumor, mice that died of a rechallenge tumor before the primary tumor were censored with respect to primary tumor-related survival.

Radiotherapy

RT was delivered to primary tumors on day 1 of treatment using an Xstrahl Small Animal Radiation Research Platform (Suwanee, Georgia, USA). Mice were immobilized using custom lead jigs that exposed the dorsal right flank as previously described.⁵ For all experiments, a maximum dose of 12 Gy RT was delivered to the right flank tumor in one fraction.

Antibodies and IC

Hu14.18-IL2 IC was provided by Apeiron Biologics (Vienna, Austria) and has been previously described.¹⁰ Intratumoral (IT) injections of 25 µg hu14.18-IL2 IC in 100 µL PBS were delivered once daily for 5 days (days 6–10). Anti-mouse-CTLA-4 mAb (IgG2c isotype of the 9D9 clone) was provided by Bristol-Myers Squibb (Redwood City, California, USA) and was administered intraperitoneally (IP) at a dose of 200 µg in 0.2 mL PBS on days 6, 9, and 12 as previously described.⁴ Anti-mouse-CD40 mAb was obtained from the ascites of nude mice injected with FGK 45.5 hybridoma cells producing agonistic anti-CD40 antibody (gift from Fritz Melchers, PhD, Basel Institute for Immunology, Basel, Switzerland). After enrichment for IgG, anti-CD40 mAb was administered IP at a dose of 500 µg in 0.2 mL PBS on day 3. CpG-1826 oligodeoxynucleotide (TCCTATGACGTCCCTGACGTT) was purchased from TriLink Biotechnologies (San Diego, California, USA) or Integrated DNA Technologies (Coralville, Iowa, USA) and administered IT at a dose of 50 µg in 0.1 mL PBS on days 6, 8, and 10. Treatment timing was selected based on previous studies.^{4–6}

Depletion experiments

Depletion of NK cells was performed with IP injection of 100 µg anti-NK1.1 mAb (clone PK136, Bio X Cell, Lebanon, New Hampshire, USA) in 0.5 mL PBS on days –1, 3, 7, and 11. Depletion of T-cells was performed with IP injection of 400 µg anti-CD4 mAb (clone GK1.5, Bio X Cell) in 0.5 mL PBS and 400 µg anti-CD8 mAb (clone 2.43, Bio X Cell) in 0.5 mL PBS on days –1, 3, 7, and 11. Confirmation of depletion efficiency was performed via whole blood flow cytometry on day 1 (online supplemental figure 1).

MHC-I induction by IFN-γ

Expression of MHC-I antigens (H-2Kb and H-2Db) was assessed by flow cytometry using H-2Db-PE (clone KH95) and H-2Kb-BV711 (clone AF6-88.5) antibodies, both obtained from BioLegend (San Diego, California, USA). Induction of MHC-I expression *in vitro* was measured by flow cytometry following a 48-hour incubation in media containing 100 U/mL IFN-γ. Induction of MHC-I

expression *in vivo* was measured by flow cytometry analysis of tumors harvested 7 days following the start of CAIR.

Flow cytometry

Mice were sacrificed on day 13 following initiation of radio-immunotherapy, and tumors were resected for analyses by flow cytometry or quantitative PCR (qPCR). Resected tumors were mechanically dissociated for 45 min using a gentleMACS dissociator (Miltenyi Biotec, Bergisch Gladbach, Germany) in HBSS supplemented with 1 mg/mL collagenase type D and 100 µg/mL DNase I (Sigma Aldrich, St. Louis, Missouri, USA) to obtain single cell suspensions.⁶ Ghost Dye Red 780 (Tonbo Biosciences, San Diego, California, USA) was used for viability staining. For cell surface staining, cells were preincubated with mouse Fc block (clone 2.4G2, BD Biosciences). After blocking, the cells were labeled with CD3-PE-Cy5 (clone 145–2 C11, BioLegend), CD4-PE-Dazzle594 (clone GK1.5, BioLegend), CD8a-APC-R700 (clone 53–6.7, BioLegend), CD25-BB515 (clone PC61, BD Biosciences, Franklin Lakes, New Jersey, USA), CD45-BV510 (clone 30-F11, BioLegend), GD2-APC (clone 14G2a, BioLegend), CD11b-BB700 (clone M1/70, BD Biosciences), F4/80-PE (clone BM8, BioLegend), Ly6G-BB711 (clone 1A8, BioLegend), and NK1.1-BV421 (clone PK136, BioLegend). Cells were then fixed and permeabilized overnight using Foxp3/Transcription Factor Staining Buffer Set (eBioscience). FoxP3 staining was then performed prior to flow cytometry (FoxP3-PE-Cy7, clone FJK-16s, BioLegend). Flow cytometry data were acquired using an Attune NxT Flow Cytometer (Thermo Fisher Scientific, Waltham, Massachusetts, USA) and analyzed using FlowJo V.10.7.1 (FlowJo LLC, Ashland, OR). The flow cytometry gating strategy is shown in online supplemental figure 2.

RNA isolation and complementary DNA synthesis

RNA was isolated using a Trizol/RNeasy (Qiagen, Gilden, Germany) Hybrid protocol using Phase Lock Gels. In brief, cells were cultured in six-well plates as described. To harvest RNA, media was aspirated from each well and 1 mL of Trizol (Thermo Fisher Scientific) was added. After a 5 min incubation, cells were scraped with a sterile scraper, and lysates were transferred to Phase Lock tubes and incubated for 5 min at RT. Chloroform (200 µL) was added to each tube followed by vigorously shaking for 15 s. Samples were centrifuged at 12,000 × g for 10 min at 4°C. Supernatants were transferred to a new tube, and an equal volume of 100% ethanol was added to each sample and gently mixed. Samples were then transferred to RNeasy columns (RNeasy Mini Kit, Qiagen) and RNA was isolated according to kit instructions. RNA was eluted in 30 µL of RNase-free water into a 1.5 mL tube and stored at –80°C. complementary DNA was synthesized from 500 ng of RNA using SuperScript IV VILO MasterMix (Thermo Fisher Scientific) following the manufacturers protocol, followed by dilution in nuclease-free water 1:10 and then stored at –20°C.

qPCR

The quantification of RNA was performed using TaqMan Fast Advanced Master Mix (Thermo Fisher Scientific) containing TaqMan primers (H2-K1/H2-D1, Assay ID: Mm04208017_mH; Tap1, Assay ID: Mm00443188_m1; Tap2, Assay ID: Mm01277033_m1; PSMB9, Assay ID: Mm00479004_m1; B2m, Assay ID: Mm00437762_m1; NLRC5, Assay ID: Mm01243039_m1). Amplification of test genes were normalized to three internal control genes: Actb (Mm00607939_s1), Gdph (Mm99999915_g1), and Hprt (Mm00446968_m1). qPCR was conducted at 50°C for 2 min, 95°C for 2 min, followed by 40 cycles of 95°C for 2 s and 60°C for 20 s. The threshold crossing value was noted for each transcript and normalized to the internal controls. The relative quantitation of each messenger RNA (mRNA) was performed using the comparative CT method. Experiments were performed using a QuantStudio 6 RealTime Flex PCR System (Thermo Fisher Scientific).

Statistical analysis

Tumor growth was monitored after treatment, and figures show the means and standard errors of the tumor volume. Results from each mouse were summarized by the time-weighted average (area under the volume-time curve, calculated using trapezoidal method). Time-weighted averages were compared between treatment groups overall by Kruskal-Wallis tests. If significance was found using the Kruskal-Wallis test, then pairwise comparisons were conducted using Mann-Whitney tests. No p value corrections were applied to the pairwise tests. Complete responders (cured mice) were defined as mice who had zero-volume tumors on the last day of the study and were alive. If significance was found using the χ^2 test, then pairwise comparisons were conducted using proportion tests. Survival curves were generated using the Kaplan-Meier method and compared using log-rank tests. For qPCR data, statistical comparisons were performed on the dCT values and analyzed via one-way analysis of variance with Šidák's multiple comparisons test. Data are presented as fold-change compared with the parental 9464D expression. Cell quantification from flow cytometry and immunohistochemistry was compared using Mann-Whitney tests. All experiments were performed in duplicate. P values less than 0.05 were considered statistically significant and are indicated in figures as *** $p < 0.001$; ** $p < 0.01$; * $p < 0.05$; NS, non-significant ($p > 0.05$). All analyses were performed using GraphPad Prism (GraphPad) or R V.4.0.5 (R Foundation for Statistical Computing).

RESULTS

CAIR treatment is effective in small 9464D-GD2 tumors and is associated with some toxicity

We previously described a combination radio-immunotherapy regimen (CAIR) that is effective in 9464D-GD2 tumors (figure 1A).⁴ We confirmed that this regimen is effective in prolonging survival ($p < 0.01$) and curing mice bearing small (50 mm³) 9464D-GD2 tumors (4/5 mice tumor free, figure 1B). Larger (100 mm³) 9464D-GD2 tumors had

prolonged survival ($p = 0.03$) but were not cured by CAIR (0/5 mice tumor free, figure 1C). In addition, we confirmed that cured mice fail to reject rechallenge with 9464D-GD2 on the contralateral flank (figure 1D), although the growth of the rechallenged tumors is slower than tumor growth in paired naïve age-matched mice ($p = 0.01$). In addition to limited efficacy against larger 9464D-GD2 tumors, CAIR is associated with moderate toxicity. To determine which components of the regimen are responsible for efficacy and toxicity, we tracked weight and survival of variants of the regimen (figure 1E). For all three regimens, following the addition of other agents to RT, we observed substantial weight loss from days 5–10. We observed similar efficacy under these conditions when anti-CTLA4 was omitted, suggesting that alleviation of immune suppression by T regulatory cells is not required for CAIR efficacy in this model. Individual tumor growth curves for the data included in figure 1E are shown in online supplemental figure 3A. These findings demonstrate that while CAIR can cure a significant number of mice bearing small 9464D-GD2 tumors, there is significant potential for improvement which might be informed by further examination of the mechanisms driving CAIR efficacy.

NK cells play a significant role in CAIR-mediated tumor cures but are not required for early tumor regression

To determine which immune subsets are involved in the response to CAIR for 9464D-GD2, we assessed treatment response in immunodeficient mice and mice depleted of specific immune subsets. We first tested the response to CAIR in immunodeficient R2G2 mice, which lack T, B, and NK cells and have decreased macrophages, dendritic cells, and neutrophils. These 9464D-GD2 tumor-bearing R2G2 mice had superior tumor response with CAIR compared with RT treated or vehicle controls ($p < 0.01$ and $p < 0.01$, respectively, figure 2A). However, after this initial reduction in tumor size during the first ~30 days following CAIR, the majority of R2G2 mice had tumor regrowth/escape by 100 days after the start of therapy (0/7 mice tumor free, figure 2A). Immunocompetent C57BL/6 mice treated with CAIR also had improved tumor response relative to RT treated or vehicle controls ($p < 0.01$ and $p < 0.01$, respectively, figure 2B), though the majority of mice were cured (4/5 mice tumor free). Individual tumor growth curves are shown in online supplemental figure 3B. These data demonstrate that early response to CAIR by 9464D-GD2 tumors is not driven by T, B, or NK cells and suggest, conversely, that late tumor control might depend on one or more of the populations of cells deficient in R2G2 mice.

To determine whether NK or T cells were responsible for preventing delayed outgrowth, and enabling cures of tumors treated with CAIR, we next performed antibody depletion experiments (figure 2C, online supplemental figure 1). As in previous experiments, 9464D-GD2 tumors treated with vehicle controls or radiation grew substantially during the first 30 days. In contrast, tumors treated with CAIR or CAIR with NK, T, or NK and T cell depletion regressed with superimposable growth curves

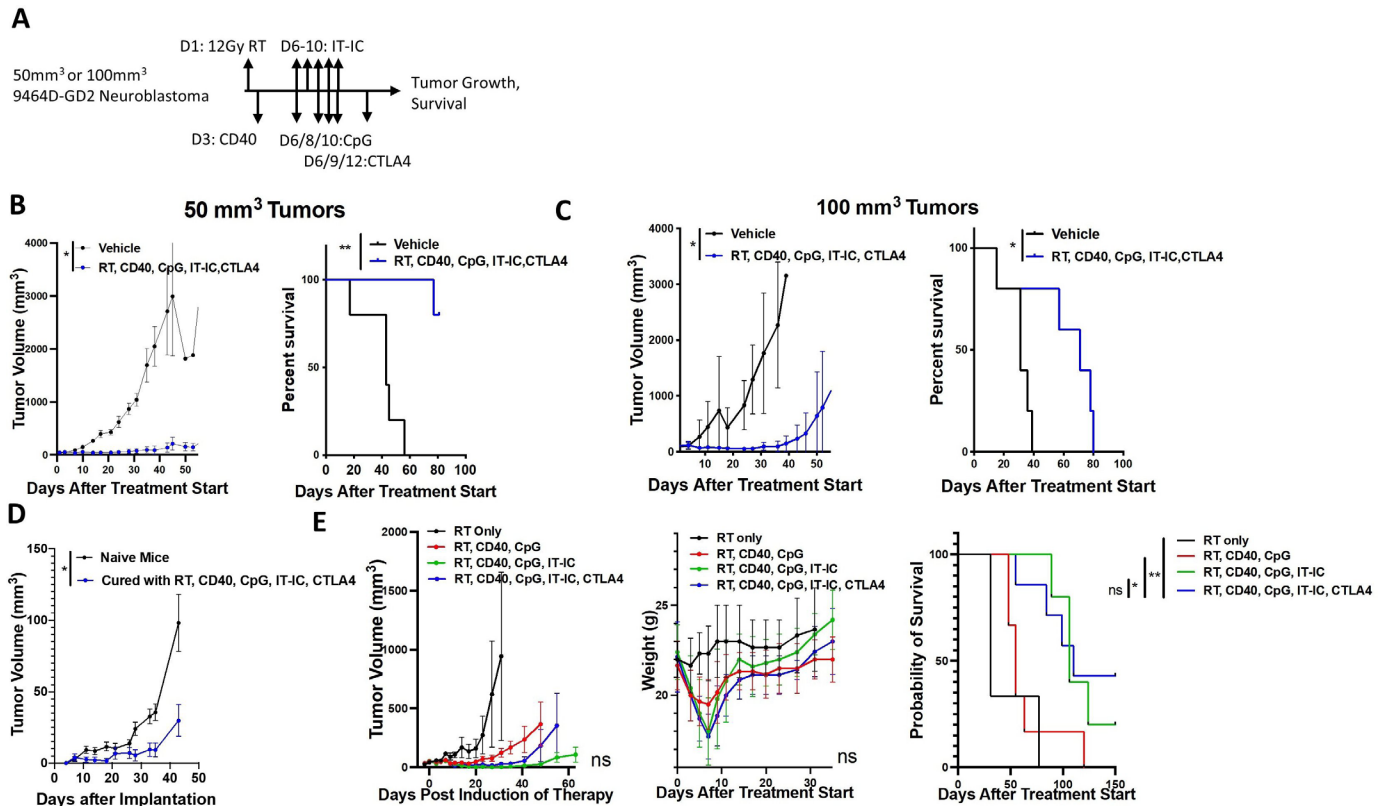


Figure 1 Combination radio-immunotherapy against 9464D-GD2 neuroblastoma tumors: some small tumors are cured, but not larger tumors. Intradermal 9464D-GD2 neuroblastoma tumors were untreated or treated with RT, IT-IC, anti-CD40, CpG, and anti-CTLA4. (A) Treatment schema of combination immunotherapy approach. (B–C) Tumor growth and survival of 50 mm³ (B) or 100 mm³ (C) 9464D-GD2 neuroblastoma tumors. (D) Mice cured of their primary tumor by CAIR were rechallenged in the contralateral flank with 9464D-GD2 neuroblastoma, along with simultaneous implantation of 9464D-GD2 into naïve mice; tumor growth over 60 days is shown. (E) Tumor growth, mouse weight, and survival in mice bearing 9464D-GD2 tumors and treated with CAIR or regimens omitting various components of the CAIR regimen. All experiments performed in duplicate and a representative single experiment is shown. CAIR, combination adaptive-innate immunotherapy regimen; IC, immunocytokine; IT, intratumoral; NS, non-significant; RT, radiation therapy. *, $p < 0.05$; **, $p < 0.01$; ***, $p < 0.001$.

during this period (figure 2D, online supplemental figure 3C), confirming that NK and T cells are not responsible for early tumor regression. However, while roughly half of CAIR-treated, non-depleted, mice developed lasting tumor cures, all mice depleted of both NK and T cells developed tumor outgrowth and were culled (figure 2E–F). Similarly, nearly all CAIR-treated mice depleted of only NK cells also showed delayed tumor outgrowth in this late period, resulting in significantly decreased survival compared with CAIR-treated IgG controls ($p < 0.05$). CAIR-treated mice depleted of only T cells followed a similar pattern as those depleted of NK cells, but the survival difference was not statistically significant compared with IgG controls ($p = 0.16$).

NK cell activity in tumors is regulated by a variety of receptor-ligand interactions, including the binding of inhibitory receptors (KIRs in humans and Ly49 in mice) to cognate MHC-I molecules.¹¹ In light of the data indicating that NK cells have a significant role in CAIR-mediated tumor cures, we hypothesized that 9464D-GD2 cells might express very low levels of MHC-I, allowing for NK cell-mediated elimination of tumors.

9464D-GD2 cells fail to express MHC-I in response to IFN- γ

MHC-I molecules play multiple roles in the interactions between cancer cells and infiltrating immune cells. In addition to NK cell inhibition, MHC-I expression by cancer cells is required for CD8⁺ T cells to recognize cognate antigens at the tumor site after priming by antigen presenting cells in draining lymph nodes. To determine the role of tumor MHC-I in the immune response to CAIR, we assessed MHC-I expression on parental 9464D and 9464D-GD2 cells *in vitro*. We found that the 9464D cells express very little surface MHC-I at baseline; however, following stimulation with IFN- γ , a potent cytokine known to induce MHC-I through ligation with its receptor IFN- γ R, roughly 25% of cells express significant levels of its two murine MHC-I genes, H-2Db and H-2Kb (figure 3A). Conversely, 9464D-GD2 expressed very little MHC-I both at baseline and after incubation with IFN- γ (figure 3B). This difference indicates that when cells from the parental cell line were transfected to express GD2, a subclone lacking MHC-I inducibility was unintentionally selected to generate the new cell line. To determine the source of MHC-I presentation dysfunction,

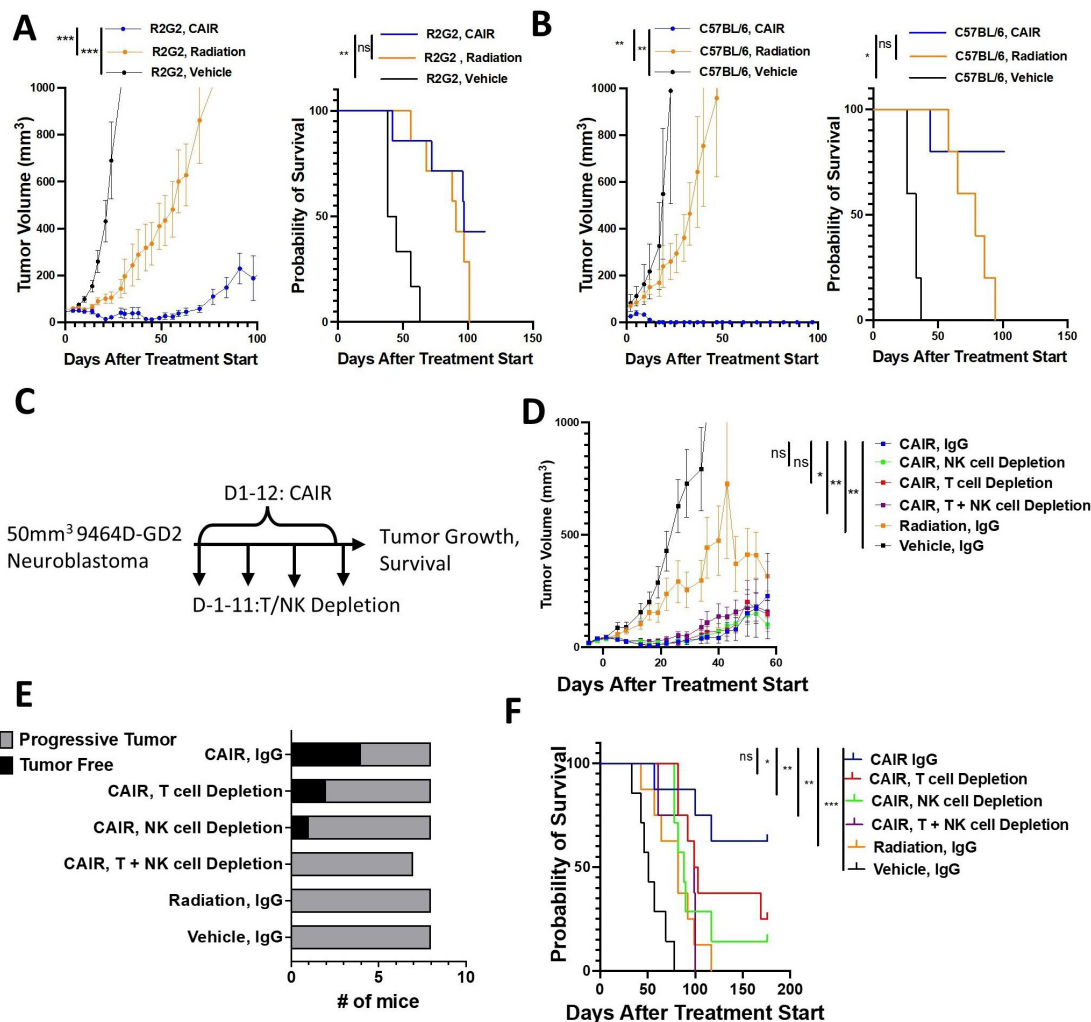


Figure 2 Late response and clearance of 9464D-GD2 is dependent on NK cells. (A) Tumor growth and survival of R2G2 mice bearing 9464D-GD2 tumors treated with CAIR. (B) Tumor growth and survival of C57BL/6 mice bearing 9464D-GD2 tumors treated concurrent to R2G2 mice with CAIR shown in figure 2A. (C) Treatment schema and depletion schedule for CAIR. (D) Tumor growth of mice treated with CAIR and concurrent T and/or NK cell depletion. (E) Number of mice in each group that developed a progressive tumor vs remaining tumor-free for the mice shown in (D). (F) Survival for mice shown in (D). All experiments performed in duplicate and a representative single experiment is shown. CAIR, combination adaptive-innate immunotherapy regimen; NK, natural killer; NS, non-significant; *, $p < 0.05$; **, $p < 0.01$; ***, $p < 0.001$.

transcription of genes related to antigen presentation and MHC expression was quantified in both 9464D and 9464D-GD2 (figure 3C). Accordingly, we observed that TAP1 and PSMB9 transcription was not upregulated in 9464D-GD2 cells following incubation with IFN- γ , in contrast to the prominent upregulation of both of these when the parental 9464D cell line was incubated with IFN- γ . TAP1 and PSMB9 share a common bi-directional promoter in humans and mice, suggesting that regulation of this promoter region might contribute to the lack of MHC-I inducibility in 9464D-GD2 cells.^{12 13}

MHC-I expressing 9464D-GD2 cells are resistant to tumor cure by CAIR

CD8⁺ T cells are unable to recognize and respond to tumor cells that do not have MHC-I expression. To assess the impact of tumor cell expression of MHC-I on responsiveness to CAIR, we developed a separate cell line from

a subclone of the parental 9464D cell line capable of upregulating MHC-I in response to IFN- γ by transfecting it to express GD2 and GD3 synthases (9464D-GD2-I) (figure 4A). To confirm that 9464D-GD2-I expression of MHC-I could be induced *in vivo*, we examined these tumor cells by flow cytometry after *in vivo* growth followed by CAIR treatment. We observed that 9464D-GD2-I, but not 9464D-GD2, effectively upregulated expression of MHC-I in response to treatment in mice (figure 4B). To determine if this difference in MHC-I induction correlated with tumor infiltration of NK or CD8⁺ T cells, we harvested tumors 13 days after the start of CAIR treatment. We found that in both 9464D-GD2-I and 9464D-GD2 tumors, CD8⁺ T cell infiltration in CAIR-treated mice increases as a percentage of live cells (figure 4C). Similarly, both types of CAIR-treated tumors appeared to have increased infiltration of NK cells at this time point, although the shift was

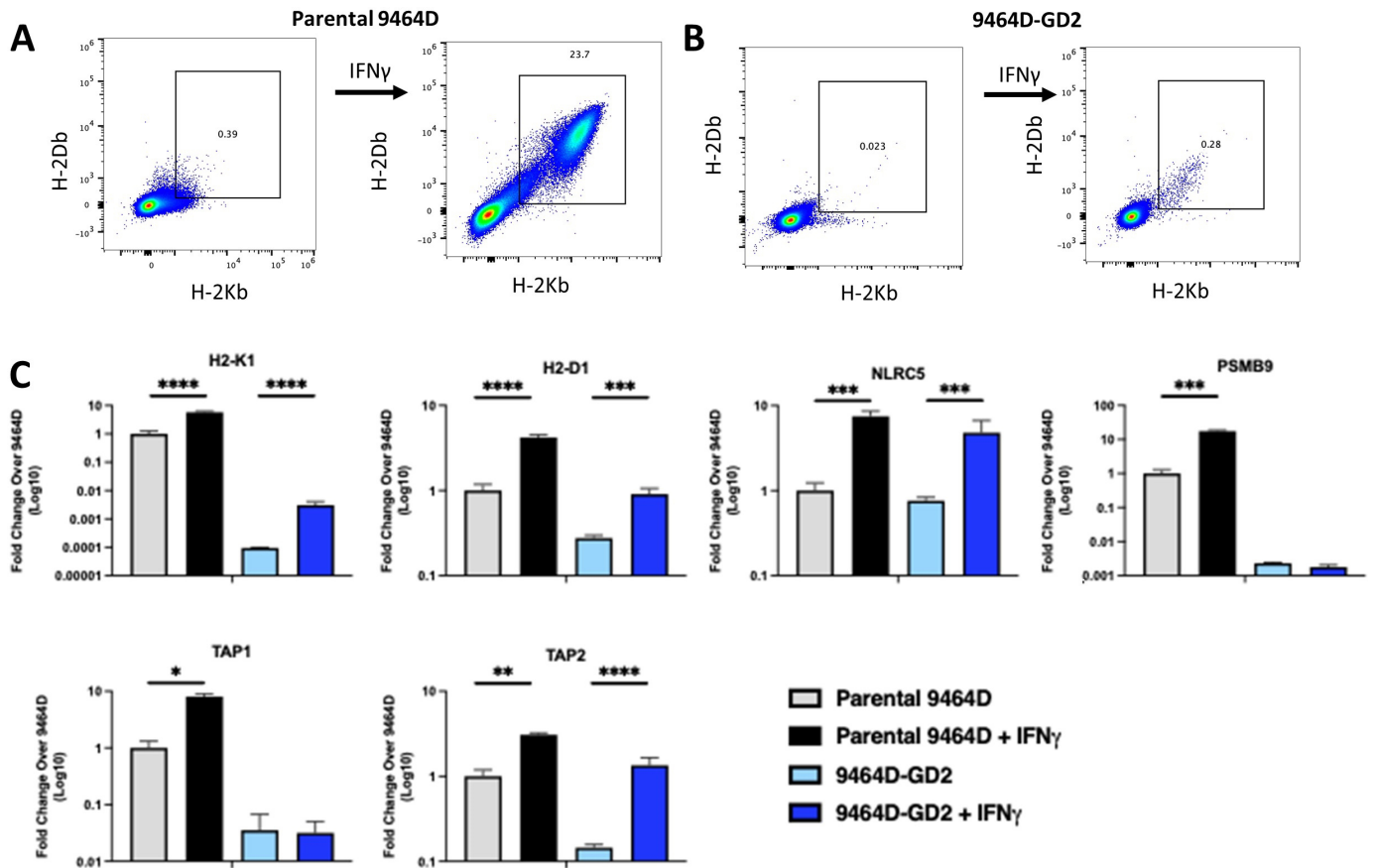


Figure 3 9464D-GD2 neuroblastoma cells do not express MHC-I in the absence or presence of stimulation by IFN- γ . (A–B) MHC-I H-2Kb and H-2Db expression in parental 9464D (A) and 9464D-GD2 (B) cells *in vitro* as assessed by flow cytometry with or without IFN- γ . (C) Quantification of quantitative reverse transcription PCR analysis of MHC-I expression machinery in parental 9464D and 9464D-GD2 cells, with and without 48-hour stimulation with IFN- γ . All experiments performed in duplicate and a representative single experiment is shown. IFN, interferon; MHC-I, major histocompatibility complex class I.

not statistically significant in 9464D-GD2 tumors. These data indicate that while MHC-I inducibility is retained *in vivo* in 9464D-GD2-I and its expression is upregulated in response to CAIR, tumor recruitment or retention of NK and T cells is not necessarily enhanced by this difference compared with the MHC-I non-inducible 9464D-GD2 tumors.

To assess if MHC-I upregulation correlated with increased responsiveness of GD2-expressing 9464D tumors to CAIR, we monitored tumor growth and survival in response to treatment (figure 4D–F). As before, we observed that both 9464D-GD2-I and 9464D-GD2 tumors showed similar regression in the first 30 days after treatment initiation, suggesting that MHC-I does not impact the early response of tumors to CAIR (figure 4E). However, after this early period, tumor growth diverged and mice bearing 9464D-GD2-I tumors had fewer cured mice than mice bearing 9464D-GD2 tumors (6/17 mice vs 13/19 mice tumor free, $p < 0.05$, figure 4D). Additionally, 9464D-GD2-I tumors regrew more quickly and had worse survival than 9464D-GD2 tumors (figure 4E–F, online supplemental figure 4), suggesting that tumor-reactive cells which are typically suppressed by MHC-I expression (NK cells and possibly macrophages) are responsible for

slowing the growth of recurrent tumors.¹⁴ Together, these data support the conclusion that NK cells, rather than CD8⁺ T cells, drive 9464D-GD2 responsiveness to CAIR and that this NK response is aided by low or absent MHC-I expression on tumor cells.

DISCUSSION

The results of this study provide insights regarding the mechanism of our recently described combination radioimmunotherapy regimen targeting innate and adaptive immunity (CAIR) in the immunologically cold 9464D-GD2 model of neuroblastoma. The initial response (substantial tumor shrinkage up through 30 days) does not appear to be mediated by NK or T cell populations. In contrast, NK cells are substantially involved in tumor cures by CAIR and might have a role in slowing tumor regrowth after recurrence. This finding is consistent with our observation that MHC-I is not expressed by 9464D-GD2 tumor cells *in vitro* or *in vivo*, and thus would not be expected to interfere with NK function via ligation of inhibitory Ly-49 receptors.¹⁵ When CAIR was applied in mice bearing tumors capable of MHC-I induction (9464D-GD2-I), the treatment was similarly effective in causing initial tumor

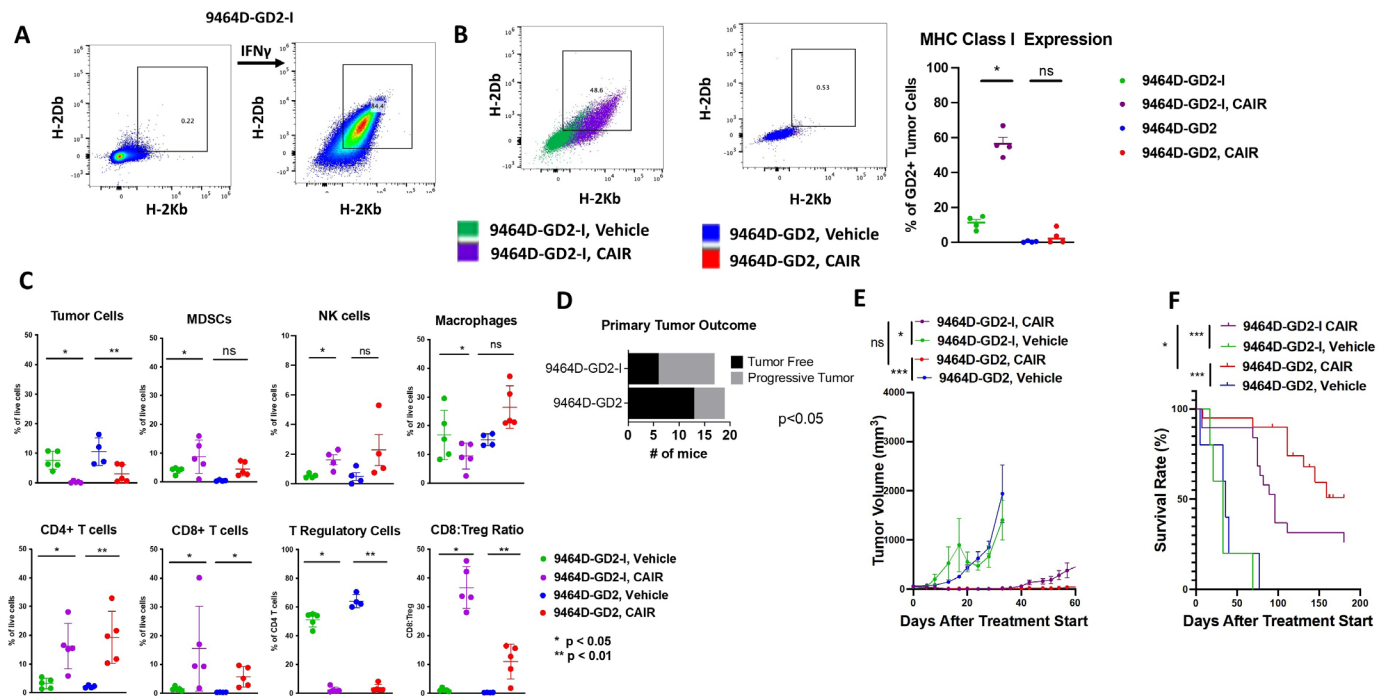


Figure 4 Selection and characterization of MHC-I inducible cell line (9464D-GD2-I) from parental 9464D. (A) *In vitro* comparison of MHC-I H-2Kb and H-2Db expression in 9464D-GD2-I cells in response to 48-hour stimulation with IFN- γ . (B) *In vivo* comparison of MHC-I H-2Kb and H-2Db expression in 9464D-GD2-I and 9464D-GD2 tumors in response to CAIR (RT, IT-IC, anti-CD40, CpG, anti-CTLA4) on day 13 of therapy. (C) The immune infiltrate of 9464D-GD2-I and 9464D-GD2 tumors untreated or treated with CAIR as assessed by flow cytometry of tumor disaggregates. (D) Treatment outcome, based on number of tumor-free mice, of 9464D-GD2-I and 9464D-GD2 tumors treated with CAIR (RT, IT-IC, anti-CD40, CpG, anti-CTLA4) shown in (E). (E) Tumor growth of treated and untreated 9464D-GD2-I and 9464D-GD2 tumors. (F) Survival of treated and untreated mice bearing 9464D-GD2-I or 9464D-GD2 tumors shown in (D and E). All experiments performed in duplicate and a representative single experiment is shown. CAIR, combination adaptive-innate immunotherapy regimen; IC, immunocytokine; IFN, interferon; IT, Intratumoral; MHC-I, major histocompatibility complex class I; NS, non-significant; RT, radiation therapy. *, $p < 0.05$; **, $p < 0.01$; ***, $p < 0.001$.

shrinkage; however, CAIR was significantly more effective at clearing tumors completely and slowing tumor outgrowth in mice bearing the MHC-I non-inducible 9464D-GD2 tumors than for mice with the MHC inducible 9464D-GD2-I tumors. These differences might be explained by the inhibition of NK cell function, a primary effector population, by MHC-I, combined with the insufficiency of the regimen to generate an effective CD8⁺ T cell response to fill in the gap in antitumor immune activity against the 9464D-GD2-I tumors.

MHC-I expression is absent or very low in nearly all high-risk clinical neuroblastoma tumors and is thought to contribute to an immunosuppressive tumor microenvironment.^{16 17} One study demonstrated that primary human neuroblastomas are similarly associated with low expression of antigen presentation machinery.¹⁸ Another study of human neuroblastoma cell lines found that of 11 commonly used cell lines, 9 expressed very low levels of mRNA related to antigen presentation on MHC-I.¹⁹ This lack of MHC expression on human neuroblastomas may be driven in part by MYCN amplification, which is associated with high-risk disease and with low expression of MHC-I and poor infiltration of T cells into the tumor microenvironment.^{20 21} Similarly, the MYCN-overexpressing preclinical mouse models of neuroblastoma, such as 9464D and

other TH-MYCN driven models, have previously been shown to express low levels of MHC-I and be minimally infiltrated by T cells.²² In some neuroblastoma cell lines with low baseline MHC-I expression, MHC-I expression can be induced by IFN- γ stimulation.^{18 23} However, this does not necessarily improve treatment response. While potentially increasing T cell recognition, induction of MHC-I has been shown to result in decreased sensitivity to NK-mediated cytotoxicity.¹⁸ Accordingly, we have previously demonstrated that upregulation of MHC-I on NXS2 neuroblastoma cells can mediate escape from NK-driven immunotherapy *in vivo* by inhibiting NK cell function.¹⁵

Expression of antigens on MHC-I molecules is an intricate process requiring cleavage of intracellular proteins by the proteasome or immunoproteasome, translocation of peptides through TAP channels in the endoplasmic reticulum (ER) membrane, trimming of peptides in the ER, and loading of high-affinity peptides before translocation to the cell surface. As a result, interference with any of these steps can inhibit cell surface expression of MHC-I. Common methods of MHC-I downregulation by tumors include epigenetic dysregulation of genes relating to antigen presentation and, more rarely, selection for mutations of these genes.²⁴ Through a mechanism not yet understood, the data presented here demonstrate that

expression of TAP1 and PSMB9, genes responsible for cleavage and translocation of peptides into the ER, are dysregulated in 9464D-GD2. Similarly, loss of TAP1 and PSMB9 induction has been linked to the loss of MHC-I expression in models of renal cell carcinoma and leiomyosarcoma.^{25,26} Expression of these genes is linked by a common bi-directional promoter that is induced by IFN- γ via IRF2 and STAT1.^{12,27} Accordingly, defects in the IFN- γ response pathway have also been linked to loss of MHC-I expression by cancer cells.²⁸ It is not yet clear if the lack of TAP1 and PSMB9 inducibility by IFN- γ is solely, or directly, responsible for low MHC-I expression on 9464D-GD2 or how expression of these genes is dysregulated. Future studies will aim to clarify this association and identify the mechanism by which TAP1 and PSMB9 are suppressed in 9464D-GD2. Further analyses of the regulation of these pathways, possibly via epigenetic modulation, may help determine whether this observation has relevance for human disease and potential therapeutic strategies to engage CD8⁺ T cells.^{29–32}

In this study we demonstrated that early regression of 9464D-GD2 and 9464D-GD2-I tumors following CAIR treatment was not solely mediated by radiotherapy, indicating that the initial response is driven by the immunotherapy component of CAIR. We demonstrated that NK and T cells were not required for early tumor response, suggesting that non-lymphocyte populations drive the early antitumor response of these tumors to CAIR. Previously, we published a study showing that CD40 agonism combined with CpG, two components of CAIR, can mediate tumor regression via infiltration of tumoricidal macrophages and macrophage repolarization.^{33–35} Our prior report also demonstrated that anti-CD40 and/or CpG are required for the responsiveness of 9464D-GD2 tumors to CAIR, suggesting that this mechanism might play a role in curing 9464D-GD2 tumors.⁴ Preliminary data from ongoing studies in our lab are suggestive of a potential role for macrophages in the early response to this CAIR regimen. Further work is underway to address this question in a separate report.

Even though the tumor response data demonstrate that T cells are not required in the early tumor response to CAIR, analysis of immune cells infiltrating into these tumors show an increase in infiltrating CD4⁺ and CD8⁺ T cells correlating with the increase in infiltrating NK cells. The increased infiltration of lymphocyte populations into tumors after CAIR suggests that this treatment results in the secretion of chemokines, which is driven by pro-inflammatory signaling. This pro-inflammatory environment may be aided in part by the demonstrated depletion of T regulatory cells by CAIR, likely by the anti-CTLA4 component of the regimen. Taken together, these results indicate that while T cells may not have a significant role in the early tumor response, CAIR treatment drives their recruitment, suggesting that corresponding induction of MHC-I with additional alleviation of immune suppression might further support antitumor T cell activity. Thus, the role of anti-CTLA4, which does not appear to have a

significant role in tumor shrinkage in this model, might change substantially if further changes are made to the CAIR regimen that increase the T cell mediated anti-tumor effect.

Conclusion

We show here that in the 9464D-GD2 model of neuroblastoma, NK cells are a primary effector population driving tumor cures and slowing tumor escape from our combination radio-immunotherapy regimen, CAIR. This conclusion is supported by reduced efficacy of CAIR after antibody depletion of NK cells and the finding that the inducible expression of MHC-I in 9464D-GD2-I corresponds to fewer tumor cures and more rapid tumor outgrowth. Future studies should explore the role of myeloid cells in the treatment response, the ability to potentially modulate MHC class-I expression *in vivo* to drive an effective CD8⁺ T cell response, and the relevance of this model to human disease.

Author affiliations

¹Department of General Surgery, University of Wisconsin Hospitals and Clinics, Madison, Wisconsin, USA

²Department of Human Oncology, University of Wisconsin-Madison, Madison, Wisconsin, USA

³Provenance Biopharmaceuticals, Carlisle, Massachusetts, USA

⁴Biosstatistics and Medical Informatics, University of Wisconsin-Madison, Madison, Wisconsin, USA

⁵Department of Pediatrics, University of Wisconsin-Madison, Madison, Wisconsin, USA

Contributors TA performed experiments, analyzed and interpreted data, and was the primary author of this manuscript. AE, ASF, and LZ designed and conducted experiments representing multiple figures in the manuscript. DK, MR, and AS assisted in animal studies, including drug administration and tumor measurements. ASF and AE assisted in flow cytometry. JB assisted with statistical analyses. SDG originally created the immunocytokine and the antibody studied. TA, AE, ALR, ZM, and PMS were key contributors to the experimental concept and design. PMS was the guarantor of the study. All authors contributed to the writing of the manuscript and approved the final manuscript.

Funding This work was supported by Midwest Athletes Against Childhood Cancer; Stand Up 2 Cancer; the St. Baldrick's Foundation; the Crawdaddy Foundation; the University of Wisconsin Carbone Cancer Center, and the Children's Neuroblastoma Cancer Foundation. This research was also supported in part by public health service grants T32 CA090217, U54-CA232568, R35-CA197078, U01-CA233102, and Project 3 of P01CA250972 from the National Cancer Institute; and UL1TR002373 from the National Institutes of Health and the Department of Health and Human Services. Shared resource flow cytometry reagents and equipment are funded by University of Wisconsin Carbone Cancer Center Support Grant P30-CA014520. The content is solely the responsibility of the authors and does not necessarily represent the official views of the National Institutes of Health.

Competing interests SDG declares employment and ownership interests in Provenance Biopharmaceuticals.

Patient consent for publication Not applicable.

Provenance and peer review Not commissioned; externally peer reviewed.

Data availability statement Data are available upon reasonable request.

Supplemental material This content has been supplied by the author(s). It has not been vetted by BMJ Publishing Group Limited (BMJ) and may not have been peer-reviewed. Any opinions or recommendations discussed are solely those of the author(s) and are not endorsed by BMJ. BMJ disclaims all liability and responsibility arising from any reliance placed on the content. Where the content includes any translated material, BMJ does not warrant the accuracy and reliability of the translations (including but not limited to local regulations, clinical guidelines,

terminology, drug names and drug dosages), and is not responsible for any error and/or omissions arising from translation and adaptation or otherwise.

Open access This is an open access article distributed in accordance with the Creative Commons Attribution Non Commercial (CC BY-NC 4.0) license, which permits others to distribute, remix, adapt, build upon this work non-commercially, and license their derivative works on different terms, provided the original work is properly cited, appropriate credit is given, any changes made indicated, and the use is non-commercial. See <http://creativecommons.org/licenses/by-nc/4.0/>.

ORCID iDs

Taylor J Aiken <http://orcid.org/0000-0003-1139-9822>

Alexander L Rakhmievich <http://orcid.org/0000-0002-2686-9500>

Paul M Sondel <http://orcid.org/0000-0002-0981-8875>

REFERENCES

- 1 Matthay KK, Maris JM, Schleiermacher G, *et al.* Neuroblastoma. *Nat Rev Dis Primers* 2016;2:16078.
- 2 Coughlan D, Gianferante M, Lynch CF, *et al.* Treatment and survival of childhood neuroblastoma: evidence from a population-based study in the United States. *Pediatr Hematol Oncol* 2017;34:320–30.
- 3 Yu AL, Gilman AL, Ozkaynak MF, *et al.* Anti-GD2 antibody with GM-CSF, interleukin-2, and isotretinoin for neuroblastoma. *N Engl J Med* 2010;363:1324–34.
- 4 Voeller J, Erbe AK, Slowinski J, *et al.* Combined innate and adaptive immunotherapy overcomes resistance of immunologically cold syngeneic murine neuroblastoma to checkpoint inhibition. *J Immunother Cancer* 2019;7:344.
- 5 Morris ZS, Guy EI, Francis DM, *et al.* *In Situ* tumor vaccination by combining local radiation and tumor-specific antibody or immunocytokine treatments. *Cancer Res* 2016;76:3929–41.
- 6 Rakhmievich AL, Felder M, Lever L, *et al.* Effective combination of innate and adaptive immunotherapeutic approaches in a mouse melanoma model. *J Immunol* 2017;198:1575–84.
- 7 Norris MD, Burkhart CA, Marshall GM, *et al.* Expression of N-myc and MRP genes and their relationship to N-myc gene dosage and tumor formation in a murine neuroblastoma model. *Med Pediatr Oncol* 2000;35:585–9.
- 8 Mombaerts P, Clarke AR, Rudnicki MA, *et al.* Mutations in T-cell antigen receptor genes alpha and beta block thymocyte development at different stages. *Nature* 1992;360:225–31.
- 9 Mazurier F, Fontanellas A, Salesse S, *et al.* A novel immunodeficient mouse model--RAG2 x common cytokine receptor gamma chain double mutants--requiring exogenous cytokine administration for human hematopoietic stem cell engraftment. *J Interferon Cytokine Res* 1999;19:533–41.
- 10 Gillies SD, Reilly EB, Lo KM, *et al.* Antibody-Targeted interleukin 2 stimulates T-cell killing of autologous tumor cells. *Proc Natl Acad Sci U S A* 1992;89:1428–32.
- 11 Sternberg-Simon M, Brodin P, Pickman Y, *et al.* Natural killer cell inhibitory receptor expression in humans and mice: a closer look. *Front Immunol* 2013;4:65.
- 12 Wright KL, White LC, Kelly A, *et al.* Coordinate regulation of the human TAP1 and LMP2 genes from a shared bidirectional promoter. *J Exp Med* 1995;181:1459–71.
- 13 Yan G, Fu Y, Faustman DL. Reduced expression of TAP1 and LMP2 antigen-processing genes in the nonobese diabetic (NOD) mouse due to a mutation in their shared bidirectional promoter. *J Immunol* 1997;159:3068–80.
- 14 Barkal AA, Weiskopf K, Kao KS, *et al.* Engagement of MHC class I by the inhibitory receptor LILRB1 suppresses macrophages and is a target of cancer immunotherapy. *Nat Immunol* 2018;19:76–84.
- 15 Neal ZC, Imboden M, Rakhmievich AL, *et al.* NXS2 murine neuroblastomas express increased levels of MHC class I antigens upon recurrence following NK-dependent immunotherapy. *Cancer Immunol Immunother* 2004;53:41–52.
- 16 Szanto CL, Cornel AM, Vijver SV, *et al.* Monitoring immune responses in neuroblastoma patients during therapy. *Cancers* 2020;12:519.
- 17 Wöfl M, Jungbluth AA, Garrido F, *et al.* Expression of MHC class I, MHC class II, and cancer germline antigens in neuroblastoma. *Cancer Immunol Immunother* 2005;54:400–6.
- 18 Raffaghello L, Prigione I, Bocca P, *et al.* Multiple defects of the antigen-processing machinery components in human neuroblastoma: immunotherapeutic implications. *Oncogene* 2005;24:4634–44.
- 19 Corrias MV, Occhino M, Croce M, *et al.* Lack of HLA-class I antigens in human neuroblastoma cells: analysis of its relationship to TAP and tapasin expression. *Tissue Antigens* 2001;57:110–7.
- 20 Layer JP, Kronmüller MT, Quast T, *et al.* Amplification of N-myc is associated with a T-cell-poor microenvironment in metastatic neuroblastoma restraining interferon pathway activity and chemokine expression. *Oncimmunology* 2017;6:e1320626.
- 21 Bernards R, Dessain SK, Weinberg RA. N-myc amplification causes down-modulation of MHC class I antigen expression in neuroblastoma. *Cell* 1986;47:667–74.
- 22 Webb ER, Lanati S, Wareham C, *et al.* Immune characterization of pre-clinical murine models of neuroblastoma. *Sci Rep* 2020;10:16695.
- 23 Lampson LA, George DL. Interferon-Mediated induction of class I MHC products in human neuronal cell lines: analysis of HLA and β 2-m RNA, and HLA-A and HLA-B proteins and polymorphic specificities. *J Interferon Res* 1986;6:257–65.
- 24 Dhatchinamoorthy K, Colbert JD, Rock KL. Cancer immune evasion through loss of MHC class I antigen presentation. *Front Immunol* 2021;12:636568.
- 25 Dovhey SE, Ghosh NS, Wright KL. Loss of interferon-gamma inducibility of TAP1 and LMP2 in a renal cell carcinoma cell line. *Cancer Res* 2000;60:5789–96.
- 26 Hayashi T, Kobayashi Y, Kohsaka S, *et al.* The mutation in the ATP-binding region of JAK1, identified in human uterine leiomyosarcomas, results in defective interferon- γ inducibility of TAP1 and LMP2. *Oncogene* 2006;25:4016–26.
- 27 Rouyez M-C, Lestingi M, Charon M, *et al.* IFN regulatory factor-2 cooperates with STAT1 to regulate transporter associated with antigen processing-1 promoter activity. *J Immunol* 2005;174:3948–58.
- 28 Jorgovanovic D, Song M, Wang L, *et al.* Roles of IFN- γ in tumor progression and regression: a review. *Biomark Res* 2020;8:49.
- 29 Ratner N, Brodeur GM, Dale RC, *et al.* The neuro of neuroblastoma: Neuroblastoma as a neurodevelopmental disorder. *Ann Neurol* 2016;80:13–23.
- 30 Ganeshan VR, Schor NF. Pharmacologic management of high-risk neuroblastoma in children. *Paediatr Drugs* 2011;13:245–55.
- 31 Ram Kumar RM, Schor NF. Methylation of DNA and chromatin as a mechanism of oncogenesis and therapeutic target in neuroblastoma. *Oncotarget* 2018;9:22184–93.
- 32 Jubierre L, Jiménez C, Rovira E, *et al.* Targeting of epigenetic regulators in neuroblastoma. *Exp Mol Med* 2018;50:1–12.
- 33 Buhtoiarov IN, Lum HD, Berke G, *et al.* Synergistic activation of macrophages via CD40 and TLR9 results in T cell independent antitumor effects. *J Immunol* 2006;176:309–18.
- 34 Rakhmievich AL, Buhtoiarov IN, Malkovsky M, *et al.* CD40 ligation in vivo can induce T cell independent antitumor effects even against immunogenic tumors. *Cancer Immunol Immunother* 2008;57:1151–60.
- 35 Buhtoiarov IN, Sondel PM, Wigginton JM, *et al.* Anti-tumour synergy of cytotoxic chemotherapy and anti-CD40 plus CpG-ODN immunotherapy through repolarization of tumour-associated macrophages. *Immunology* 2011;132:226–39.